Nanoscale

PAPER

Forced phage uncorking: viral DNA ejection triggered by a mechanically sensitive switch†

Cite this: DOI: 10.1039/c7nr05897g

Miklós S. Z. Kellermayer, Zsuzsanna Vörös, Gabriella Csík and Levente Herényi

Received 9th August 2017,
Accepted 19th December 2017

DOI: 10.1039/c7nr05897g

rsc.li/nanoscale

The foremost event of bacteriophage infection is the ejection of genomic material into the host bacterium after virus binding to surface receptor sites. How ejection is triggered is yet unknown. Here we show, in single mature T7 phage particles, that tapping the capsid wall with an oscillating atomic-force-microscope cantilever triggers rapid DNA ejection *via* the tail complex. The triggering rate increases exponentially as a function of force, following transition-state theory, across an activation barrier of 23 kcal mol^{-1} at 1.2 nm along the reaction coordinate. The conformation of the ejected DNA molecule revealed that it had been exposed to a propulsive force. This force, arising from intra-capsid pressure, assists in initiating the ejection process and the transfer of DNA across spatial dimensions beyond that of the virion. Chemical immobilization of the tail fibers also resulted in enhanced DNA ejection, suggesting that the triggering process might involve a conformational switch that can be mechanically activated either by external forces or *via* the tail-fiber complex.

Introduction

Viruses are parasitic infectious agents comprising a nanoscale shell (capsid) that encapsulates the genomic material. Most bacteriophage viruses invade bacteria by transferring their genome inside the host cell while leaving the capsid outside.[1,2] The mechanisms of viral DNA transfer have been the subject of much investigation and debate.[3–5] Theoretical considerations have pointed out the possibility of DNA pressure build-up in the viral capsid.[6–10] This pressure can in principle be utilized for the ejection of the genomic DNA during infection of the host cell. Single-molecule mechanics experiments demonstrated that the portal motor of the Φ 29 virus generates a very large force which is used to package DNA so that a pressure as large as 60 atm is built up within the capsid.[11] Real-time imaging of the dsDNA expelled from phage particles upon the binding of *E. coli* receptor protein revealed that the speed of ejection, at least in the initial phase, may be up to 75 kbp s^{-1}.[12,13] Thus, there indeed is a high initial pressure available to drive the DNA molecule out of the capsid, but the slow and steady take-up of DNA by the host cell[1,2] points at the involvement of enzymatic[3–5,14] and osmotic[4,6–10] mechanisms as well to the completion of the ejection process. Phage infection begins with the search and recognition of receptor molecules (*e.g.*, FhuA for T5,[11,13] lipopolysaccharides for T7 [12,13,15]) on the bacterial surface. Once the phage is securely bound, a series of little-understood conformational changes take place in the tail complex, which result in the formation of an ejection conduit[16] followed by the actual DNA ejection. The mechanisms of how the recognition signal is relayed, during this triggering process, through the tail, are unknown. In the case of viruses infecting eukaryotic organisms it has been shown that mechanical effects play an important role in the initial steps of capsid disassembly and genome unpacking.[17–22] In the present work we applied mechanical load on the capsid wall of surface-adsorbed T7 bacteriophage particles with an oscillating AFM cantilever. Surprisingly, mechanical force triggered the ejection of phage DNA *via* the tail, and increasing loads accelerated the triggering process.

Results and discussion

We investigated the role of mechanical force in triggering DNA ejection of the T7 bacteriophage. T7 possesses a head of icosahedral symmetry and a short, non-contractile tail.[23] Mature phages containing tightly packed 40 kbp dsDNA were used. We employed atomic force microscopy (AFM) to visualize the topographical structure and mechanically induced changes of the phage particles covalently attached to a mica surface. In AFM images of a substrate surface coated with T7 we were able to resolve the structure of the capsid and the tail (Fig. 1, Fig. S1†). The tail appeared as a cone with a mean length of

Department of Biophysics and Radiation Biology, Semmelweis University, Tűzoltó u. 37-47, Budapest H-1094, Hungary.
E-mail: kellermayer.miklos@med.semmelweis-univ.hu

† Electronic supplementary information (ESI) available: Image and data analysis, force calibration, triggering rate calculation, video. See DOI: 10.1039/c7nr05897g

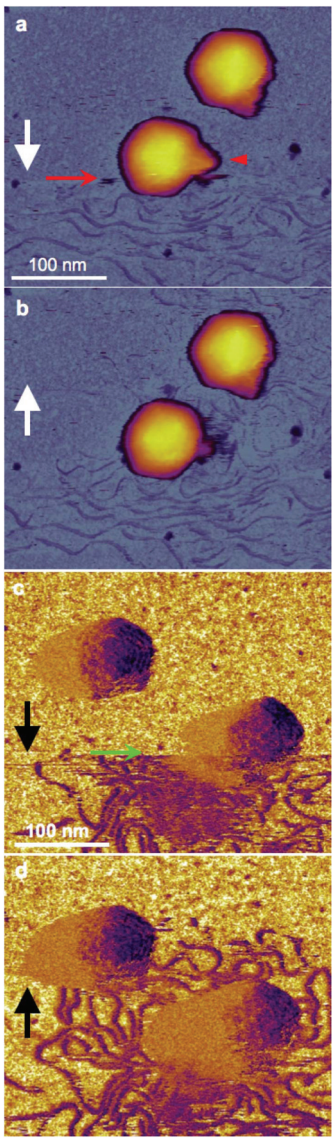

Fig. 1 *In situ* AFM of DNA ejection from the T7 bacteriophage. a, b. Sequential height-contrast AFM images collected during (a) and following (b) DNA ejection. Images are separated by 7 minutes. White arrows indicate AFM line-scanning direction. The red arrow points at the scan line in which DNA suddenly appeared. DNA molecules appear as fine, randomly coiled threads around the capsids. The red arrowhead points at the tail complex, the surface of which became fuzzy after DNA ejection. c, d. Sequential phase-contrast AFM images collected during (c) and following (d) DNA ejection. Images are separated by 8 minutes. Black arrows indicate the AFM line-scanning direction. Green arrow points at the scan line in which DNA suddenly appeared in the image. The DNA molecule can be particularly well visualized in the phase-contrast image because of its different viscoelastic properties relative to those of the substrate. The ordered regions of ejected DNA containing parallel threads indicate that the molecule was kinetically trapped on the surface.

22.8 nm (±3.0 nm S.D., n = 149, see the ESI†), which compares well with the 23 nm reported previously.[24] Interestingly, DNA, which appeared in the form of random threads bound to the poly-L-lysine-coated substrate surface, often became suddenly visible while scanning the capsid (Fig. 1a and c). The DNA molecule emerged abruptly from one AFM scan line to the next. Conceivably, the DNA was released as a consequence of mechanically tapping the capsid with the cantilever tip. The ejected DNA was particularly well resolvable in phase-contrast AFM images due to the differences in the viscoelastic properties of DNA and the substrate surface (Fig. 1c and d).

To explore the details of DNA ejection further, we carried out *in situ* AFM measurements during which image acquisition on the same capsid was continued as a function of time (Fig. 2 and ESI Video 1†). The high-spatial-resolution, time-

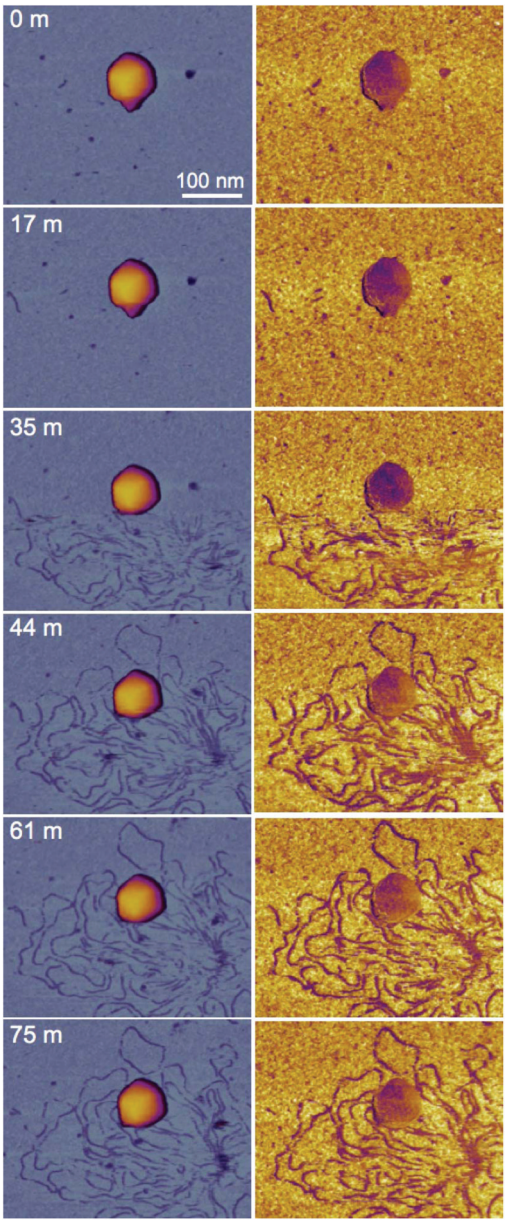

Fig. 2 *In situ* AFM of mechanically triggered DNA ejection. Height- (left column) and phase- (right column) contrast AFM images of the same T7 particle are shown. The frame size is 450 nm × 450 nm. Numbers indicate the timing of the frames in minutes. See also ESI Video 1.†

dependent AFM images allowed us to identify several key features of the mechanically driven viral DNA ejection process: (1) most of the DNA is ejected in less than 1 s considering the ~1 Hz line-scan rate compared with the within-one-linescan emergence and structural consolidation of DNA as judged from the temporal constancy of its surface arrangement following ejection (Fig. 2).

Considering the 40 kbp size of the T7 genome, our results are comparable with the 60–75 kbp s^{-1} ejection rate measured earlier,[12,13] which results in the emission of a significant portion of the viral genome. (2) The ejected and surface-adsorbed DNA is most likely a partial T7 genome in a kinetically trapped structural state. The mean diameter of the area covered with DNA was 355 nm (±57 nm S.D., n = 43, see the ESI†), which is smaller than that expected for either the surface-equilibrated (~1.3 μm) or the surface-projected total genomic T7 DNA (~0.7 μm). Furthermore, we often observed regions in which the DNA chains displayed an apparent nematic ordering (Fig. 1d). Such an ordering is unexpected for conformational equilibration of a random chain and points at the trapping of the molecule exposed to projectile forces. (3) The force-induced viral DNA ejection occurs *via* its natural path, through the tail. Although the tail complex often maintained its gross conical appearance (Fig. S10†), frequently it shrank and sometimes disappeared (Fig. 1b, 2, S11, ESI Video 1†) pointing at structural rearrangements associated with the ejection process. Furthermore, in the case of phages pointing towards the surface with their tail, DNA propulsion visibly occurred from the direction of the tail complex (Fig. 1d, 2), indicating that ejection took place forcibly through the tail. We exclude the possibility that DNA was ejected due to breaking the tail off with the cantilever tip, because even a partial mechanical tapping of the capsid body resulted in DNA release (Fig. S9, ESI Video 2†). (4) Finally, the trigger for DNA ejection is most likely a mechanical perturbation that propagates through the compressible medium of the DNA-filled capsid towards the tail complex. In support of this notion, the global structure of the capsid remained essentially intact following DNA ejection. Furthermore, the location of mechanical perturbation by the AFM cantilever in the instant of DNA ejection was different from the location of the tail (see Fig. S9, ESI Video 2†), and the perturbations caused neither a complete capsid collapse, nor a gaping hole on the surface. In sum, mechanically tapping the surface of the T7 capsid evokes a signal to trigger the ejection of its genomic DNA. Although DNA-filled viral capsids have been manipulated before with AFM to reveal their nanomechanical behavior,[25,26] such a systematic, mechanically triggered DNA ejection has so far not been reported. This discrepancy may be explained by noting that while in a nanomechanical experiment (or in jumping-mode imaging) the capsid is pressed only once and briefly, during the AFM scanning employed here the cantilever oscillates with a high frequency (often exceeding 30 kHz) and exerts a given average force on the capsid wall for an extended period of time (up to several seconds, see the ESI, Fig. S5†). Based on an independent, empirical calibration of cantilever force *versus* oscillation amplitude (Fig. S3†) we estimate that in our *in situ* AFM experiment (Fig. 1 and 2, ESI Video 1†) the capsid was pressed with an average force of ~40 pN in the instant of DNA ejection. Assuming that pressure distribution is determined by compressibility, the small indentation caused by this force (0.057 nm, see the ESI†) corresponds to a ~0.067–0.135 atm increment to the 60 atm internal pressure in the capsid.[11] Accordingly, a meager 0.1–0.2% pressure increase is sufficient to trigger DNA ejection. The persisting force on the capsid wall reduces the lifetime of the pre-ejection structural state of the virus. We note that the force applied by the cantilever is not constant but oscillatory. Whether and how the oscillatory nature contributes to triggering DNA ejection remains to be investigated. In our subsequent analysis we use the average force values provided by the calibration procedure. Conceivably, the pre-ejection-state lifetime becomes reduced because the invested mechanical energy lowers the activation barrier towards an initial intermediate state along the DNA ejection pathway. Because the reaction pathway, which likely contains further intermediate states, always ends in the DNA-ejected state, the initial, triggering transition is of key importance: once its barrier is crossed, the rest of the transitions along the reaction pathway are completed spontaneously.

To directly assess the role of force in the DNA-ejection trigger and to reveal the energetics of the triggering reaction, we exposed T7 capsids to increasing average mechanical loads and measured the ratio of the capsids that ejected their genomic DNA (Fig. 3). According to the transition-state theory, mechanical force (F) strongly influences the rate of reactions

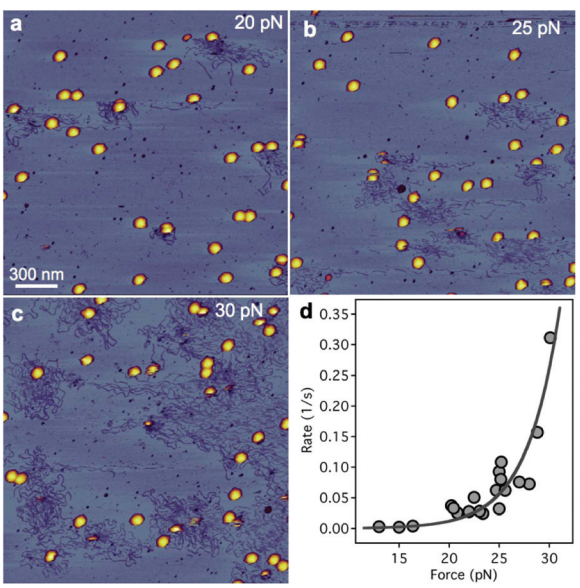

Fig. 3 Effect of increasing mechanical load on the triggering rate of DNA ejection. a. AFM scan of a 2 × 2 μm sample surface area exposed to an average force of 20 pN. b, c. AFM image of other 2 × 2 μm^2 areas of the same sample exposed to average forces of 25 and 30 pN, respectively. d. Rate of DNA ejection as a function of mechanical load. Data were fitted with eqn (1). The data points were collected in three independent experiments.

(k_F)[27] depending on the invested mechanical energy $(F\Delta x)$ relative to the activation energy (E_a) as

$$k_F = \left(Ae^{-\frac{E_a - F\Delta x}{k_B T}} = Ae^{-\frac{E_a}{k_B T}} e^{\frac{F\Delta x}{k_B T}}\right) = k_0 e^{\frac{F\Delta x}{k_B T}}, \quad (1)$$

where k_0 is the rate of the spontaneous process at constant temperature (T), Δx is a distance parameter along the reaction coordinate related to the energetic topology of the system, and k_B is Boltzmann's constant. Applying this theory we tested the effect of increasing loads on the rate of triggering T7 DNA ejection by scanning different large sample areas (2×2 μm^2) with progressively increasing forces (Fig. 3). Increasing loads resulted in the progressive appearance of DNA ejected by a mechanical trigger (Fig. 3a–c). Fitting the data with eqn (1) (Fig. 3d) revealed a spontaneous DNA ejection trigger rate of 2.6×10^{-5} s^{-1} that corresponds to an activation energy of 23 kcal mol^{-1} (see the ESI†), which compares well with earlier bulk measurements (20–40 kcal mol^{-1}).[4] Whether force increases or decreases the rate of a reaction depends on its orientation relative to the direction of the reaction coordinate. In our experiments force was applied on the capsid wall, but DNA ejection occurred *via* the tail, which is some distance away from the point of attack. Thus, the mechanical perturbation caused by the cantilever is relayed, as pressure, *via* the continuum of the capsid wall and the semi-crystalline DNA, towards the tail complex. We obtained 1.2 nm for the distance parameter Δx, which corresponds to the expected structural change within the tail related to triggering. The exact nature of this structural change is yet unknown. The exponential dependence of triggering rate on force is manifested in a very sharp force response that acts as a sensitive mechanical switch: while below ~20 pN the rate is negligible, above this force triggering takes place rapidly (Fig. 3d). The triggering rates observed at these forces exceed the lipopolysaccharide-induced tail channel opening rate measured recently for T7 (~4.2×10^{-4} s^{-1}),[15] suggesting that triggering DNA ejection is indeed very sensitive to mechanical force.

The ejected DNA is highly unevenly distributed with regard to the capsid ejecting it (Fig. 4a), indicating that the ejection process generates a local propulsion carrying the expelled molecule across the viscous medium. The distance, as measured here, may far exceed the dimensions of the capsid. While from these experiments it is difficult to estimate the forces the ejected molecule was exposed to, it is clear that the forces are sufficient to carry the genomic material of the bacteriophage through distances beyond the thickness of the bacterial wall. Even though it is evident that pressure is present in the capsid, its role is unclear in the case of T7, because its DNA has been shown to be ejected into the host *via* an enzymatic mechanism.[14] Notably, globular particles with an average size of 5.0 nm (±1.5 nm S.D., n = 81) were also observed in the vicinity of the ejected DNA molecule (Fig. 4b, S8†). While the exact characterization of the particles is not possible with conventional methods (*e.g.*, electrophoresis and western blotting) due to the singularity of the force-driven process, we speculate that they correspond to the viral core

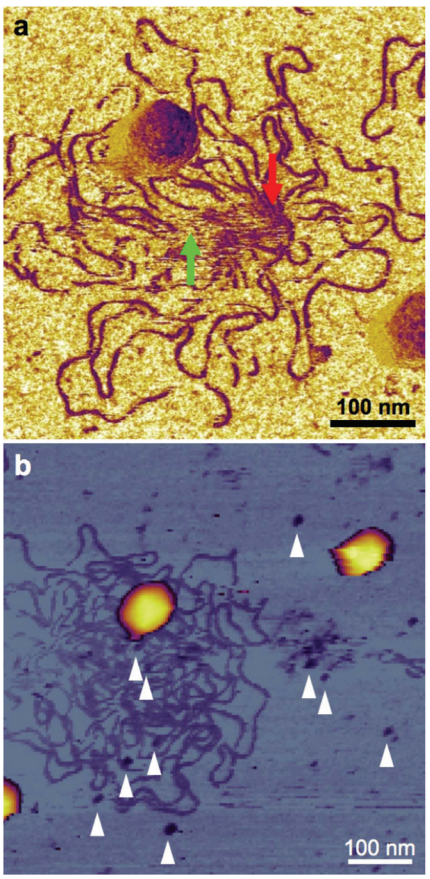

Fig. 4 Analysis of viral material ejected upon mechanical trigger. a. AFM image of the ejected and surface-adsorbed genomic DNA. Phase-contrast AFM image is shown. Green and red arrows point at the center of DNA mass and the maximum of DNA density, respectively. b. Globular particles (marked by white arrowheads) in the vicinity of the ejected DNA molecule. For further information, see the ESI.†

proteins gp14, gp15 and gp16, which are ejected prior to DNA and are thought to contribute to the ejection conduit.[16,24] It is an intriguing possibility that the mechanical energy stored in the encapsulated DNA is utilized towards the unfolding and ejection of the core proteins and towards the construction and maintenance of the conduit. Such a mechanism might be relevant in all the phages with short, non-contractile tails. Furthermore, the internal pressure likely contributes to mechanically pre-loading the ejection machinery, thereby tilting the energy landscape towards DNA ejection; in this state a small additional force is sufficient to trigger the process with an apparently switch-like mechanism.

To explore the possible mechanisms behind the switch-like step, we chemically fixed (with 5% glutaraldehyde) the T7 phage sample following the phages covalent binding to the surface (Fig. 5) (see the ESI†). We anticipated that such a fixation step would completely abolish DNA ejection because of the structural stabilization of the capsid wall. To our surprise, the substrate surface was already populated with DNA by the time of AFM scanning, indicating that the fixation actually

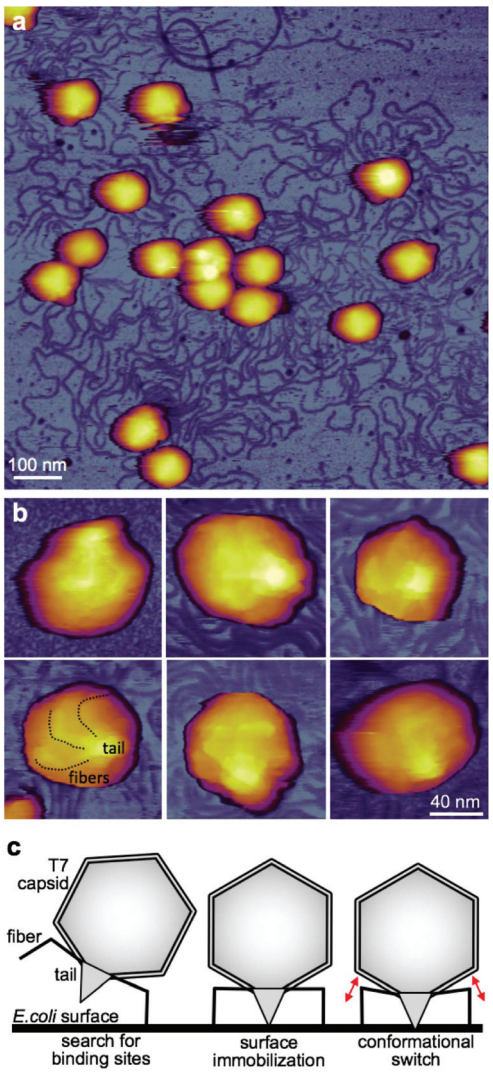

Fig. 5 Investigation of chemically fixed T7 phage particles. a. AFM image of T7 phage particles covalently attached to a poly-L-lysine-coated and glutaraldehyde-treated mica surface. The sample was chemically fixed with 5% glutaraldehyde following surface binding. b. High-resolution magnified AFM images of T7 particles with their tail complex pointing away from the substrate surface, hence towards the viewer. Dotted lines in the bottom left image guide the eye along the fibers immobilized on the capsid surface. c. Schematic model of T7 binding to the *E. coli* surface and passing through a switching step prior to genomic DNA release. Red double arrows indicate the putative conformational switch thought to be associated with a change in the fiber arrangement.

resulted in enhanced triggering of DNA ejection (Fig. 5a). We note that fixation-induced DNA release from T7 has been observed before.[28,29] Remarkably, the tail fibers of the T7 phages, which are difficult to clearly identify in the unfixed preparations, became visible on the surface of the capsids (Fig. 5b). Thus, most plausibly it is the surface immobilization of the tail fibers that results in a DNA trigger similarly to the action of mechanical forces. Hypothetically, the immobilization of the tail fibers induces a conformational switching (Fig. 5c) that triggers DNA ejection just as in the case of mechanical force. The details of the conformational switch and the fixation-induced DNA ejection are yet unknown. The processes might involve a lever-like action of the tail fibers that results in a transition within the tail complex. Intriguingly, the same series of events can be triggered by force.

Our experiments allowed a direct visualization of the ejection of dsDNA from a viral capsid upon mechanical trigger. The forces employed here cause very small changes in the internal pressure of the capsid, yet are sufficient to trigger DNA ejection. Thus, a DNA-filled capsid is in a state poised for expelling its genomic material and the proteins required for the faithful execution of the initial steps of phage infection. It is of particular interest that the induced pressure changes are oscillatory; similar pressure oscillations, created by ultrasound exposure, for example, might in principle be employed for a selective viral DNS-ejection trigger under bulk conditions. Considering the emerging interest in artificial micro- and nanocapsules capable of triggered material release,[30] understanding how viral DNA ejection is triggered carries important application potential. The unique features of the single-particle mechanics method employed here may be useful in uncovering the fine details of viral DNA ejection.

Experimental

T7 bacteriophages (ATCC 11303-B7) were grown in *E. coli* (ATCC 11303) and purified according to published methods.[31] The phage suspension was concentrated on a CsCl gradient and dialyzed against buffer (20 mM Tris-HCl, 50 mM NaCl, pH 7.4).[32] T7 bacteriophage concentration was determined from optical density by using an extinction coefficient of $\varepsilon_{260} = 7.3 \times 10^3$ (mol nucleotide bases per L per cm). T7 samples diluted in PBS (137 mM NaCl, 2.7 mM KCl, 10 mM Na_2HPO_4, 1.8 mM KH_2PO_4, pH 7.4) were applied to mica functionalized glutaraldehyde for covalent attachment.[33] Briefly, freshly cleaved mica was first incubated with poly-L-lysine (0.01% aqueous solution) for 20 minutes at room temperature, then rinsed extensively with Milli-Q water and dried with a stream of high-purity N_2 gas. Subsequently, the surface was incubated with 10% aqueous glutaraldehyde for 30 minutes at room temperature, then rinsed extensively with Milli-Q water and dried with a stream of high-purity N_2 gas. Finally, a sample of T7 phage was loaded onto the substrate surface and incubated for 40 minutes on ice. Unbound viruses were removed by gentle washing with PBS. Considering that divalent cations may stabilize T7,[32] in some experiments we added 1 mM $MgCl_2$ with no difference in the results. When investigating chemically fixed T7 particles, glutaraldehyde treatment (5%) was carried out after the surface attachment of the capsids. Non-contact mode AFM images were acquired with an Asylum Research Cypher ES instrument (Asylum Research, Oxford Instruments, Santa Barbara, CA) by using silicon-nitride cantilevers (Olympus BL-AC40TS-C2). 512 × 512-pixel images were collected at a typical line scanning frequency of 0.2–1.5 Hz.

Cantilever speed was maximum at 1 μm s^{-1}. Cantilever resonance was excited with the photothermal method (BlueDrive™)[34] at frequencies, depending on individual cantilever tuning, between 20 and 27 kHz. Accordingly, a T7 particle was tapped up to 1600 times in a typical line scan (up to 260 times per pixel). Nominal free cantilever oscillation amplitude was 100 mV and the setpoint was varied between 70 and 90 mV. The temperature was kept constant at 20 °C with a precision of 0.1 °C. Height contrast images were corrected for flatness of field. The height contrast images were displayed with custom-written color look-up tables in order to indicate local contrast on both the substrate and the capsid surfaces. AFM images were processed and analyzed with the built-in algorithms of the driver software. Data analysis was carried out by using IgorPro program (v6.34, Wavemetrics, Lake Oswego, OR).

Conclusions

In summary, upon gently tapping the capsid wall of the T7 bacteriophage with an atomic force microscope cantilever, the virus rapidly ejected its DNA. At increasing mechanical loads the rate of triggering DNA-ejection increased exponentially according to the transition-state theory. By varying the mechanical load we obtained important insights into the energetic topology of the triggering process. Our results indicate that DNA ejection is controlled by a sensitive conformational switch that can be activated by mechanical force.

Conflicts of interest

Q3 ■■■■

Acknowledgements

This work was supported by grants from the Hungarian National Research, Development and Innovation Office (K109480; K124966; VKSZ_14-1-2015-0052; NVKP-16-1-2016-0017 National Heart Program). The research leading to these results has received funding from the European Union's Seventh Framework Program (FP7/2007-2013) under grant agreement no. HEALTH-F2-2011-278850 (INMiND).

Notes and references

1 A. D. Hershey and M. Chase, *J. Gen. Physiol.*, 1952, **36**, 39–56.
2 D. Van Valen, D. Wu, Y.-J. Chen, H. Tuson, P. Wiggins and R. Phillips, *Curr. Biol.*, 2012, **22**, 1339–1343.
3 P. Grayson and I. J. Molineux, *Curr. Opin. Microbiol.*, 2007, **10**, 401–409.
4 I. J. Molineux and D. Panja, *Nat. Rev. Microbiol.*, 2013, **11**, 194–204.
5 I. J. Molineux, *Virology*, 2006, **344**, 221–229.
6 J. Kindt, S. Tzlil, A. Ben-Shaul and W. M. Gelbart, *Proc. Natl. Acad. Sci. U. S. A.*, 2001, **98**, 13671–13674.
7 T. Odijk, *Biophys. J.*, 1998, **75**, 1223–1227.
8 P. K. Purohit, M. M. Inamdar, P. D. Grayson, T. M. Squires, J. Kondev and R. Phillips, *Biophys. J.*, 2005, **88**, 851–866.
9 P. K. Purohit, J. Kondev and R. Phillips, *Proc. Natl. Acad. Sci. U. S. A.*, 2003, **100**, 3173–3178.
10 S. Tzlil, J. T. Kindt, W. M. Gelbart and A. Ben-Shaul, *Biophys. J.*, 2003, **84**, 1616–1627.
11 D. E. Smith, S. J. Tans, S. B. Smith, S. Grimes, D. L. Anderson and C. Bustamante, *Nature*, 2001, **413**, 748–752.
12 P. Grayson, L. Han, T. Winther and R. Phillips, *Proc. Natl. Acad. Sci. U. S. A.*, 2007, **104**, 14652–14657.
13 S. Mangenot, M. Hochrein, J. Rädler and L. Letellier, *Curr. Biol.*, 2005, **15**, 430–435.
14 P. Kemp, M. Gupta and I. J. Molineux, *Mol. Microbiol.*, 2004, **53**, 1251–1265.
15 V. A. González-García, M. Pulido-Cid, C. Garcia-Doval, R. Bocanegra, M. J. van Raaij, J. Martín-Benito, A. Cuervo and J. L. Carrascosa, *J. Biol. Chem.*, 2015, **290**, 10038–10044.
16 B. Hu, W. Margolin, I. J. Molineux and J. Liu, *Science*, 2013, **339**, 576–579.
17 I. Banerjee, Y. Miyake, S. P. Nobs, C. Schneider, P. Horvath, M. Kopf, P. Matthias, A. Helenius and Y. Yamauchi, *Science*, 2014, **346**, 473–477.
18 K. H. Bremner, J. Scherer, J. Yi, M. Vershinin, S. P. Gross and R. B. Vallee, *Cell Host Microbe*, 2009, **6**, 523–535.
19 C. J. Burckhardt, M. Suomalainen, P. Schoenenberger, K. Boucke, S. Hemmi and U. F. Greber, *Cell Host Microbe*, 2011, **10**, 105–117.
20 A. Ortega-Esteban, A. J. Pérez-Berná, R. Menéndez-Conejero, S. J. Flint, C. S. Martín and P. J. de Pablo, *Sci. Rep.*, 2013, **3**.
Q4
21 A. Ortega-Esteban, K. Bodensiek, C. San Martín, M. Suomalainen, U. F. Greber, P. J. de Pablo and I. A. T. Schaap, *ACS Nano*, 2015, **9**, 10571–10579.
22 S. Strunze, M. F. Engelke, I.-H. Wang, D. Puntener, K. Boucke, S. Schleich, M. Way, P. Schoenenberger, C. J. Burckhardt and U. F. Greber, *Cell Host Microbe*, 2011, **10**, 210–223.
23 M. E. Cerritelli, J. F. Conway, N. Cheng, B. L. Trus and A. C. Steven, *Adv. Protein Chem.*, 2003, **64**, 301–323.
24 I. J. Molineux, *Mol. Microbiol.*, 2001, **40**, 1–8.
25 A. Evilevitch, W. H. Roos, I. L. Ivanovska, M. Jeembaeva, B. Jönsson and G. J. L. Wuite, *J. Mol. Biol.*, 2011, **405**, 18–23.
26 I. Ivanovska, G. Wuite, B. Jönsson and A. Evilevitch, *Proc. Natl. Acad. Sci. U. S. A.*, 2007, **104**, 9603–9608.
27 E. Evans and K. Ritchie, *Biophys. J.*, 1997, **72**, 1541–1555.
28 P. Serwer, *J. Ultrastruct. Res.*, 1978, **65**, 112–118.
29 P. Serwer, *J. Mol. Biol.*, 1976, **107**, 271–291.
30 W.-C. Liao, C.-H. Lu, R. Hartmann, F. Wang, Y. S. Sohn, W. J. Parak and I. Willner, *ACS Nano*, 2015, **9**, 9078–9086.

31 J. H. Strauss and R. L. Sinsheimer, *J. Mol. Biol.*, 1963, **7**, 43–54.
32 K. Tóth, G. Csik and G. Y. Rontó, *Physiol. Chem. Phys. Med. NMR*, 1987, **19**, 67–74.
33 H. Wang, R. Bash, J. G. Yodh, G. L. Hager, D. Lohr and S. M. Lindsay, *Biophys. J.*, 2002, **83**, 3619–3625.
34 A. Labuda, J. Cleveland and N. A. Geisse, *Microsc. Microanal.*, 2014, **28**, S21–S25.